Journal of Electroceramics, 14, 171–175, 2005

Phase Decomposition and Dielectric Properties of Reactively Sputtered Bismuth Zinc Niobate Pyrochlore Thin Films Deposited from Monoclinic Zirconolite Target

KYUNG HYUN KO, DONG HYUK BACK, YOUNG PYO HONG & JOONG HO MOON
Department of Materials Science and Engineering, Ajou University, Suwon 443-749, South Korea

Submitted February 27, 2004; Revised October 20, 2004; Accepted October 21, 2004

Abstract. Thin films of Bi_2O_3-ZnO-Nb_2O_5 system with cubic pyrochlore structure can be deposited using both cubic and monoclinic (zirconolite) targets. When monoclinic target was used, the as-deposited phase was nonequilibrium cubic monophase. After post-annealing in the 600–800°C range, phase decomposition occurred, resulting in more thermodynamically stable cubic pyrochlore and monoclinic zirconolite phases. The dielectric properties, such as dielectric constant and electric field dependent tunability, showed a steep increase along with phase separation. However, dielectric loss had a reverse tendency. The maximum tunability was about 38%, which exceeds that of cubic pyrochlore monophase films deposited from cubic target.

Keywords: tunability, sputtering, dielectric properties, pyrochlore

1. Introduction

Tunable dielectric materials for microwave voltage tunable applications, such as broadband mobile communication, have been introduced successfully. Among them, most efforts have focused on investigations of ferroelectric materials like $SrTiO_3$, $(Ba_{1-x}Sr_x)TiO_3$ [1–9]. However, ferroelectric thin films inherently have larger dielectric losses than paraelectric materials due to capacitive hysteresis in the microwave region. On account of this, Bi_2O_3-ZnO-Nb_2O_5 (BZN) pyrochlore system was suggested as another proper candidate not only because of its paraelectric properties but also because of its high dielectric constant, low losses and low co-firing temperature. There are two main phases in the BZN system depending on composition; $(Bi_{3x}Zn_{2-3x})(Zn_xNb_{2-x})O_7$, where $x = 1/2$ for cubic pyrochlore and $x = 2/3$ for monoclinic zirconolite structures (space group C2/c), respectively [10, 11].

It has been reported that BZN films prepared by metal organic deposition (MOD) process [12–14], pulsed laser deposition (PLD) [15, 16] and RF-magnetron sputtering [17–19] showed noticeable voltage-tunable dielectric properties. Recently, it was found that one of the most important factors for tunability is nonstoichiometry of the BZN films (especially Bi contents) when cubic BZN target is used [12, 13]. In this work, the dielectric-tunable properties of BZN thin films by RF-magnetron sputtering using monoclinic BZN target were investigated in terms of nonstoichiometry.

2. Experimental Procedure

The BZN thin films were deposited on Pt(111)/TiO_2/SiO_2/Si (1500 Å/200 Å/3000 Å/550 μm) substrates. The target materials ($Bi_2Zn_{2/3}Nb_{4/3}O_7$) were fabricated using the conventional mixed-oxide process. Bi_2O_3, ZnO, and Nb_2O_3 (High Purity Chemical Laboratory, Japan), 99.9% pure powders, were weighed in an appropriate ratio, mixed by ball-milling for 12 h, then calcined at 950°C for 2 h. The density of target was higher than 97% of theoretical density. The sputtering system used an off-axis type geometry of target to substrate and its distance was 13 cm. The base pressure in the process chamber was 3.0×10^{-6} Torr, while the working pressure was maintained

at 10 mTorr using a throttle valve. High-purity Ar (99.999%) and O_2 (99.999%) were used as base and reactive gases, respectively. Plasma discharging was generated at a constant RF power of 150 W and the gas ratio (O_2/Ar) held at 10%. The substrate temperature varied between room temperature and 600°C. Post-annealing processes were carried out at 600–800°C for 3 h in air to crystallize the films. Positioning thermally-evaporated silver dots (250 μm diameter) as the top electrode, the standard capacitor type metal-insulator-metal heterostructure devices were fabricated for measuring the dielectric properties.

The crystalline structures of thin films were characterized by X-ray diffraction (XRD, Mac Science M18XHF, Cu-Kα radiation) and TEM (Philips CM20 at 200 KV). In particular, the TEM diffraction patterns were analyzed using the SADP Indexing Tool version 2.0 (Alloy Design Lab., Dept. of Materials Engineering, Hanyang University) and DIPANA programs. The microstructures and morphologies were investigated by scanning electron microscopy (SEM, JEOL JSM-6330F) equipped with field emission. The compositions of the films were investigated with transmission electron microscopy energy dispersive X-ray spectroscopy (EDX) with TEM. The dielectric properties of the films were measured at room temperature with an Agilent 4294A precision impedance analyzer in the 40 Hz–10 MHz range with a 500 mV root-mean-square (rms) oscillation voltage. The DC-bias field for the tunable property of films was within ±40 V and the measurement frequency was 1 MHz.

3. Results and Discussion

The thickness of all as-deposited and post-annealed thin films were about 4000 Å. Although the substrate temperature was increased, the deposition rate was not

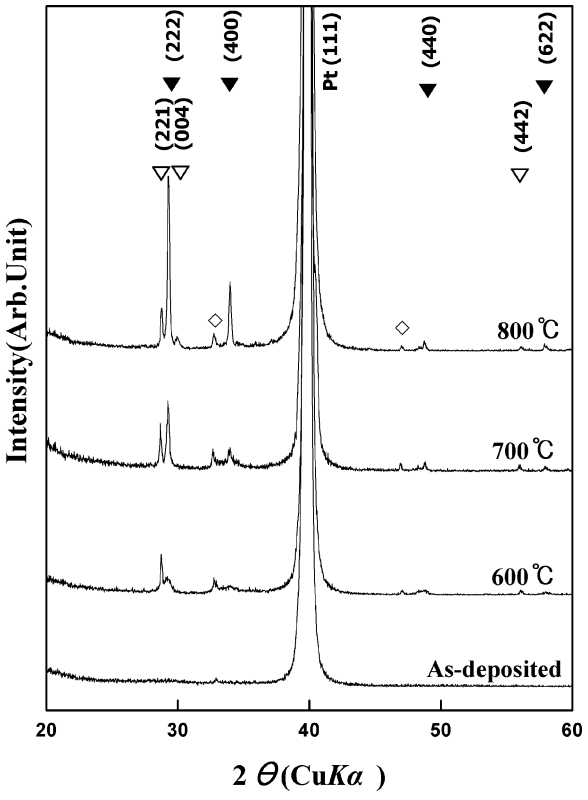

Fig. 1. XRD patterns of the BZN films deposited with substrate heating of 350°C, as a function of post-annealing temperature. (▼ = cubic phase, ∇ = monoclinic phase, ◊ = $Bi_5Nb_3O_{15}$)

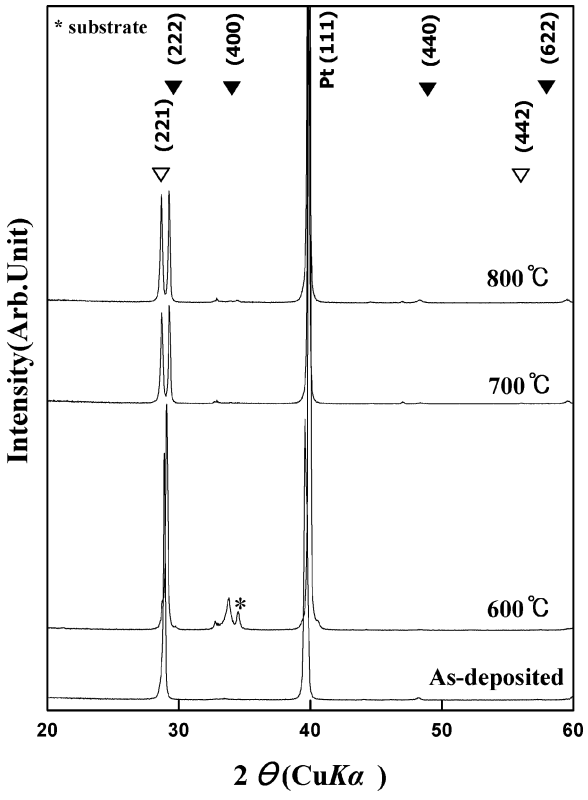

Fig. 2. XRD patterns of the BZN films deposited with substrate heating of 600°C, as a function of post-annealing temperature. (▼ = cubic phase, ∇ = monoclinic phase)

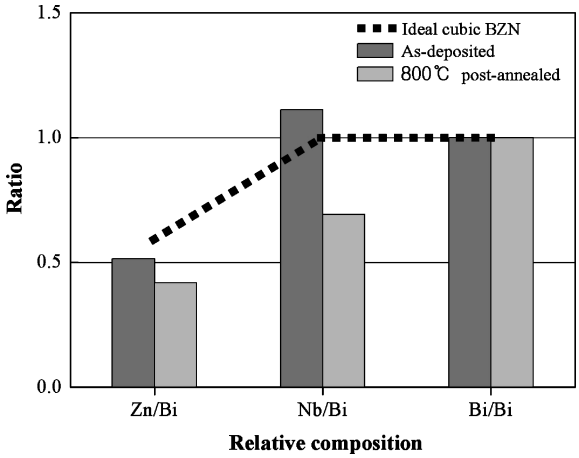

Fig. 3. EDX analysis on Zn/Bi, Nb/Bi ratio of BZN films deposited with substrate heating of 600°C, as-deposited and post-annealed at 800°C.

affected significantly. Figures 1 and 2 show the XRD patterns of as-deposited and post-annealed BZN thin films deposited with substrate heating. It was found that zinc niobate secondary phases are included in the BZN thin films deposited by $Bi_{1.5}Zn_{1.0}Nb_{1.5}O_7$ (cubic composition) target in early works [17, 18]. However, the XRD patterns for BZN thin films using monoclinic target after post-annealing at various temperatures (Figs. 1 and 2) showed that there are only small traces of bismuth niobate indexed as $Bi_5Nb_3O_{15}$ in films deposited with substrate heating of 350°C. The as-deposited films with substrate heating of 600°C consisted only of cubic phase (Fig. 2). Because the crystallization activation energy of cubic BZN phase is smaller than that of monoclinic BZN phase [20], cubic BZN phase rather than monoclinic BZN phase is supposed to form preferably at the onset of film deposition due to the quick-condensation nature of the sputtering-deposition process. The EDX results in Fig. 3 show the overall composition of as-deposited BZN films. Comparing them with the ideal stoichiometric composition (dotted lines), the composition of the films was supersaturated with respect to Nb, but close to that of cubic BZN. Therefore, this cubic phase would be in a nonequilibrium state considering chemical composition and XRD peak positions of cubic phase in the as-deposited film (Fig. 2). Apparently, it was expected that the thermodynamical restoring force from nonequilibrium would lead to a gradual decomposition of as-deposited cubic phase into a more stable cubic phase and some other phases after post-annealing. Noticing the gradual phase-separation features in Figs. 1 and 2, the nonequilibrium cubic phase started to decompose as the annealing temperature increased above 600°C, resulting in a mixed state of cubic and monoclinic phases. As separation proceeded, the lattice parameters of the cubic phase approached those of stable state. TEM diffraction pattern analysis confirmed the nature of the final mixed phases (Figs. 4 and 5). Independent of the substrate heating temperature, only two diffraction patterns corresponding to those of cubic and monoclinic were found.

In the previous work of Thayer et al. [14] demonstrated that the cubic BZN films showed wide range temperature stable tunability, but monoclinic zirconolite phase showed an unusual field dependence to the permittivity for high field at 77 K. In this study, we have focused on the room temperature dielectric properties and tunability of the BZN thin films, so all results were measured at room temperature.

Figure 6 shows the dielectric properties of the films as a function of substrate heating and post-annealing temperature. For BZN films deposited with substrate

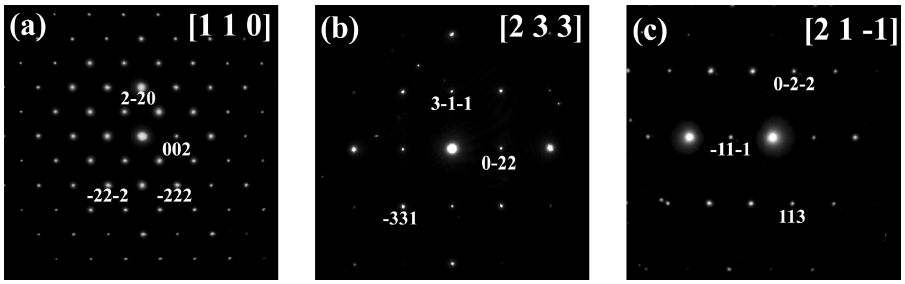

Fig. 4. Selected area diffraction patterns of the BZN films deposited with substrate heating of 350°C, post-annealed at 800°C, indexed as: (a) cubic phase, (b) cubic phase, (c) monoclinic phase.

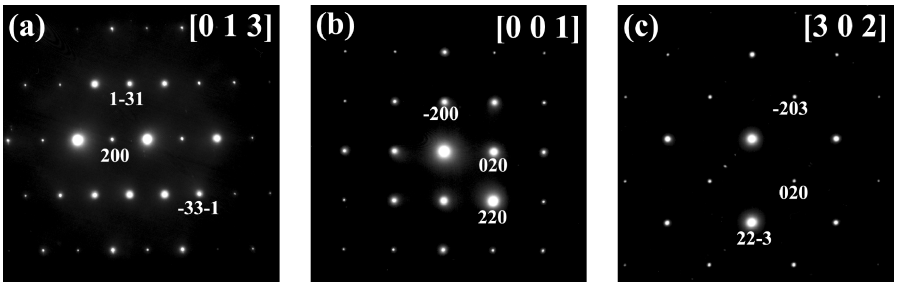

Fig. 5. Selected area diffraction patterns of the BZN films deposited with substrate heating of 600°C, post-annealed at 800°C, indexed as: (a) cubic phase, (b) cubic phase, (c) monoclinic phase.

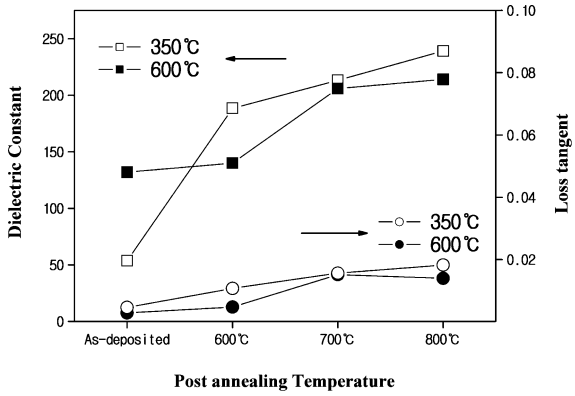

Fig. 6. Dielectric constant and loss tangent of the BZN films deposited with substrate heating of 350 and 600°C as a function of post-annealing temperature, measured at 1 MHz 500 mV oscillation voltage at room temperature.

heating of 350°C and post-annealed at 800°C, the maximum value of dielectric constant of 240 was measured. However, the dielectric losses of the films are approximately ten times as high as the previously reported values [12, 14, 17] of cubic-monophase films deposited by cubic BZN target. Furthermore, as decomposition into the dual phase of cubic and monoclinic phase proceeded, it was observed that not only the dielectric constant but also the loss tangent of the films increased significantly. It seems that newly-formed monoclinic phase by decomposition could be responsible for these trends in dielectric properties.

Field dependence of the films is shown in Fig. 7. The tunability is defined as $(C_0 - C_v)/C_0$ where C_0 and C_v are the capacitance values at zero and maximum DC-voltage levels. For a field of 1 MV/cm and a measurement frequency of 1 MHz, maximum tunability of 38% was obtained from the films deposited with substrate heating of 350°C and post-annealed at

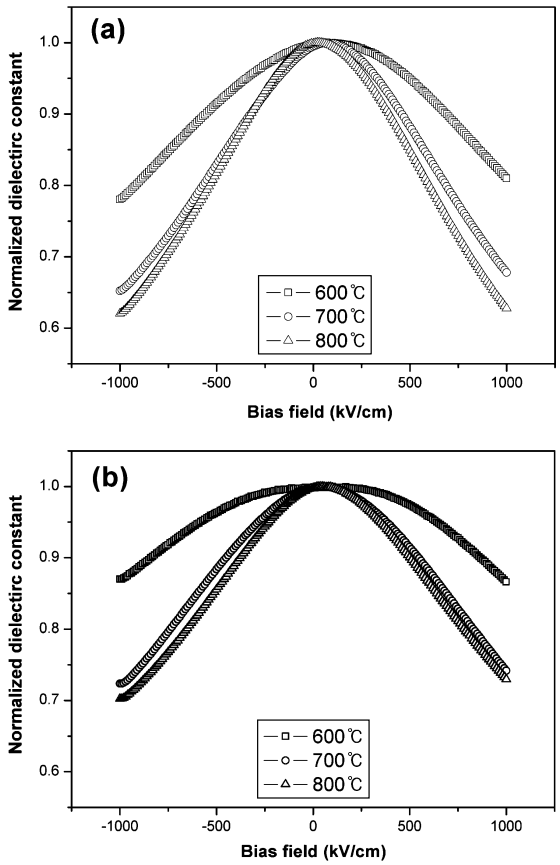

Fig. 7. Tunability of the BZN films deposited with substrate heating of (a) 350°C and (b) 600°C as a function of post-annealing temperature, measured at 1 MHz 500 mV oscillation voltage at room temperature.

800°C. Comparing our previous results concerning cubic phase deposited from cubic composition target, this tunability was found to be quite large. Considering the original target composition and the composition

analysis of films, it was conceived that the cubic phase decomposed from a supersaturated state could have a closer composition to that of the phase boundary between cubic and monoclinic than the one deposited from cubic composition target.

Regardless of substrate heating temperature, supersaturated nonequilibrium cubic phase film showed minimum tunability and quite a steep increase in tunability was observed after a vigorous start of phase separation between 600°C and 700°C (Fig. 7). However, typical field dependence on the permittivity of monoclinic (zirconolite) phase as reported in the work of Thayer et al. [14] was not observed. It is uncertain at the moment, but this may be due to a higher measuring temperature than previous reports, or the coexistence of monoclinic phase with a relatively larger amount of cubic phase.

4. Conclusions

The BZN films sputtered using target of which the composition was $Bi_2Zn_{2/3}Nb_{4/3}O_7$(monoclinic phase) consisted of single, nonequilibrium cubic phase, but decomposed into more stable cubic and monoclinic phase when post-annealing proceeded up to 800°C. The higher the substrate heating temperature, the more the portion of monoclinic phase of the films increased. The Dielectric constant and tunability of the films increased rapidly when the phase decomposition started and reached higher values than those of cubic monophase films deposited from cubic phase target.

Acknowledgments

This work was supported by the Korea Research Foundation Grant NO. KRF-2002-041-D00262.

References

1. N. Navi, H. Kim, J.S. Horwitz, H.D. Wu, and S.B. Qadri, *Appl. Phys. A*, **76**, 841 (2003).
2. X.X. Xi, H.-C. Li, W. Si, A.A. Sirenko, I.A. Akimov, J.R. Fox, A.M. Clark, and J. Hao, *J. Electroceram.*, **4**, 393 (2000).
3. W.J. Kim, W. Chang, S.B. Qadri, H.D. Wu, J.M. Pond, S.W. Kirchoefer, H.S. Newman, D.B. Chrisey, and J.S. Horwitz, *Appl. Phys. A*, **71**, 7 (2000).
4. L.C. Sengupta and S. Sengupta, *Mat. Res. Innovat.*, **2**, 278 (1999).
5. P. Padmini, T.R. Taylor, M.J. Lefevre, A.S. Nagra, R.A. York, and J. S. Speck, *Appl. Phys. Lett.*, **75**, 3186 (1999).
6. D. Fuchs, C.W. Schneider, R. Schneider, and H. Rietschel, *J. Appl. Phys.*, **85**, 7362 (1999).
7. A.B. Kozyrev, T.B. Samoilova, A.A. Golovkov, E.K. Hollmann, D.A. Kalinikos, V.E. Loginov, A.M. Prudan, O.I. Soldatenkov, D. Galt, C.H. Mueller, T.V. Rivkin, and G.A. Koepf, *J. Appl. Phys.*, **84**, 3326 (1998).
8. H.-M. Christen, L.A. Knauss, and K.S. Harshavardhan, *Materials Science and Engineering*, **B56**, 200 (1998).
9. A. Outzourhit, J.U. Trefny, T. Kito, B. Yarar, A. Naziripour, and A.M. Herman, *Thin Solid Films*, **259**, 218 (1995).
10. I. Levin, T.G. Amos, J.C. Nino, T.A. Vanderah, C.A. Randall, and M.T. Langana, *J. Solid State Chem.*, **168**, 69 (2002).
11. I. Levin, T.G. Amos, J.C. Nino, T.A. Vanderah, I.M. Reaney, C.A. Randall, and M.T. Lanagan, *J. Mater. Res.*, **17**, 1406 (2002).
12. W. Ren, S. Trolier-McKinstry, C.A. Randall, and T.R. Shrout, *J. Appl. Phys.*, **89**, 767 (2001).
13. W. Ren, R. Thayer, C.A. Randall, T.R. Shrout, and S. Trolier-McKinstry, *Mater. Res. Soc. Symp. Proc.*, **603**, 137 (2000).
14. R.L. Thayer, C.A. Randall, and S. Trolier-Mckinstry, *J. Appl. Phys.*, **94**, 1941 (2003).
15. Y.C. Chen, H.F. Cheng, Y.M. Tasu, P. Kuzel, J. Petzelt, and I.N. Lin, *J. Eur. Ceram. Soc.*, **21**, 2731 (2001).
16. H.F. Cheng, Y.C. Chen, and I.N. Lin, *J. Appl. Phys.*, **87**, 479 (2000).
17. Y. P. Hong, S. Ha, H.Y. Lee, Y.C. Lee, K.H. Ko, D.W. Kim, H.B. Hong, and K.S. Hong, *Thin Solid Films*, **419**, 183 (2002).
18. S. Ha, Y.S. Lee, Y.P. Hong, H.Y. Lee, Y.C. Lee, K.H. Ko, D.W. Kim, H.B. Hong, and K.S. Hong, *Appl. Phys. A*, **80**, 585 (2005).
19. J. Lu, Z. Chen, T.R. Taylor, and S. Stemmer, *J. Vac. Sci. Technol.*, **A21**(5), 1745 (2003).
20. S.Y. Chen, S.Y. Lee, and T.J. Lin, *J. Euro. Ceram. Soc.*, **23**, 873 (2003).